

Measuring pressure performance of a large saline aquifer during industrial-scale CO₂ injection: the Utsira Sand, Norwegian North Sea

R.A. Chadwick, G.A. Williams, J.D.O. Williams & D.J. Noy

British Geological Survey, Kingsley Dunham Centre, Keyworth, Nottingham, United Kingdom, NG 12 5GG.

Corresponding author: R.A. Chadwick e-mail: rach@bgs.ac.uk

ABSTRACT:

The Sleipner injection project has stored around 14 Mt of CO₂ in the Utsira Sand and provides a unique opportunity to monitor the pressure response of a large saline aquifer to industrial-scale CO₂ injection. There is no downhole pressure monitoring at Sleipner, but the 4D seismic programme provides an opportunity to test whether reliable indications of pressure change can be obtained from time-lapse seismic. Velocity - stress relationships for sandstones, calibrated against measured data from the Utsira Sand, indicate that pore pressure increases of <1 MPa should produce measurable travel-time increases through the reservoir. Time-lapse datasets were used to assess travel-time changes by accurately mapping the top and base of the reservoir on successive repeat surveys outside of the plume saturation footprint. Measured time-shifts are of the order of a very few milliseconds, with significant scatter about a mean value due to travel-time 'jitter'. The 'jitter' is due to non-perfect repeatability of the time-lapse surveys and shows a Gaussian distribution providing a useful statistical tool for determining the mean. Observed mean time-shifts through the Utsira Sand were 0.097 ms in 2001 and 0.175 ms in 2006. These correspond to mean pressure increases of less than 0.1 MPa. An idealised noise-free reservoir 'impulse response' was computed, taking into account lateral reservoir thickness variation. Convolution of this with the repeatability noise distribution gives a realistic predicted reservoir response. Comparing this with the observed time-shifts again indicates a pressure increase less than 0.1 MPa. Flow simulations indicate that pressure increases should range from < 0.1 MPa for an unconfined reservoir to > 1 MPa if strong flow barriers are present, so the results are consistent with the Utsira reservoir having wide lateral hydraulic connectivity.

KEYWORDS: Sleipner, CO₂ injection, pressures, saline aquifer, time-lapse seismic

1. Introduction

Capture of CO₂ from industrial point sources and long-term storage in underground geological formations (Holloway 2001) offers a viable means of contributing to an overall global warming mitigation strategy (IPCC 2007). A number of projects involving the underground storage of CO₂ are currently in progress worldwide. These range from industrial operations injecting around 1Mt of CO₂ per year, to much smaller-scale research projects injecting thousands of tonnes and aimed at learning more about reservoir processes associated with CO₂ injection. Examples of the former include natural gas processing at Sleipner in the North Sea (Baklid *et al.* 1996), at In Salah in Algeria (Riddiford *et al.* 2003) and enhanced oil recovery at Weyburn in Canada (Wilson and Monea 2004). Examples of smaller-scale projects include the Nagakoa pilot project in Japan (Kikuta *et al.* 2005) and the Frio brine project in Texas (Hovorka 2005).

These projects have demonstrated the feasibility of injecting CO₂ into subsurface geological reservoirs and are providing valuable test-beds for ongoing scientific research into issues such as time-lapse geophysical monitoring, reservoir history-matching and reaction-transport modelling etc. So far, however, a key requirement of large-scale future underground storage - the ability to inject very large volumes of CO₂ (hundreds of Mt) at high rates (5 to 20 Mt per year) - remains relatively untested. Regional-scale saline aquifers have been identified as offering the greatest ultimate potential for very large-scale CO₂ storage (Benson *et al.* 2005). The simplest estimate of the static storage capacity of an aquifer corresponds directly to the volume of available pore-space. A number of processes, however, act to reduce the efficiency with which CO₂ can replace the *in situ* formation water and render simple estimates of available pore-space volumetrics unrealistic. These processes fall into three main categories: two-phase flow effects involving the migration of the CO₂ plume itself (including capillary entry effects, residual saturations, relative permeabilities, viscous fingering etc), geochemical reactivity between the CO₂ and formation waters and minerals, and single-phase flow effects associated with the requirement to displace large volumes of water through and around the storage aquifer. The latter produces pressure increase which in some cases may be undesirably large. This issue has been addressed by a number of authors, but in particular a recent paper (Ehlig-Economides and Economides 2010) has suggested that storage reservoirs may be so strongly compartmentalised that pressure control would be prohibitively costly and large-scale CO₂ storage unfeasible.

This paper assesses evidence for pressure changes within the Utsira Sand as a consequence of the 16 year industrial-scale injection operation at Sleipner. In particular we focus on the evidence of changes in the time-lapse seismic response to pressure changes.

2. The Sleipner / Utsira injection project

Sleipner is the world's first industrial scale CO₂ injection project designed specifically as a greenhouse gas mitigation measure (Baklid *et al.* 1996). CO₂ separated from

produced natural gas is being injected into the Utsira Sand, a major saline aquifer some 26000 km² in area (Fig. 1a). Injection started in 1996 and is planned to continue for about twenty years, at a rate of nearly 1 Mt per year. CO₂ is being injected into the Utsira reservoir via a deviated (near-horizontal) well, through a 38 m-long well perforation interval ~1012 m below sea level, close to the base of the Utsira Sand, about 200 m below the reservoir top. By late 2011 around thirteen million tonnes of CO₂ had been injected.

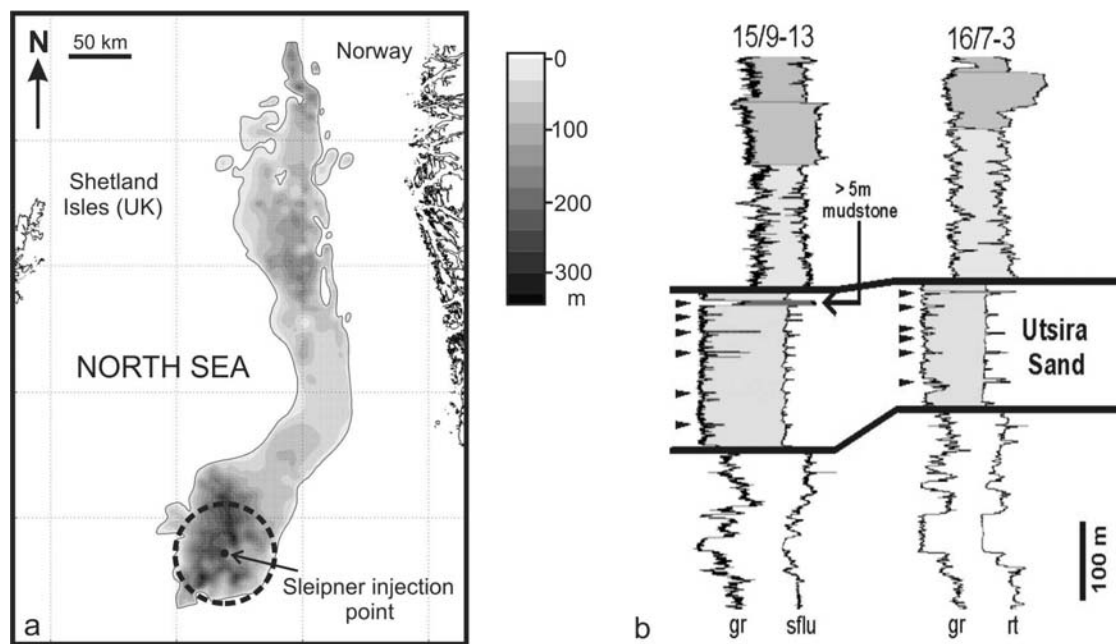


Fig. 1. a) Thickness map of the Utsira Sand and the Sleipner injection point b) Geophysical logs through the Utsira Sand showing gamma-ray (gr) peaks corresponding to intra-reservoir mudstones, reckoned to be generally ~ 1m thick (Zweigel *et al.* 2004). Dashed circle denotes 40 km radius around the injection point.

3D time-lapse seismic monitoring data (e.g. Chadwick *et al.* 2004a; Arts *et al.* 2008) image the CO₂ plume as a prominent multi-tier feature, comprising a number of bright sub-horizontal reflections, growing with time (Fig. 2). The reflections are interpreted as arising from a number of discrete layers of high saturation CO₂, each up to a few metres thick. The layers have mostly accumulated beneath very thin intra-reservoir mudstones, seen on geophysical well logs (Fig. 1b), with the uppermost layer being trapped beneath the reservoir caprock. With the exception of the topmost '5 metre mudstone' the mudstones are laterally impersistent and cannot generally be correlated from well to well. Laboratory testing of the caprock, via core samples (Harrington *et al.* 2010), indicates that it will form a satisfactory capillary seal to free CO₂.

The plume is roughly 200 m high and elliptical in plan, with a major axis approaching 4000 m by 2008. All of the individual plume reflections had formed by the time of the first time-lapse survey (1999) and have remained identifiable ever since, however the upper horizons are continuing to spread laterally and are generally maintaining

reflectivity whereas the deeper horizons have stabilized in terms of area and are becoming notably dimmer with time (Fig. 2).

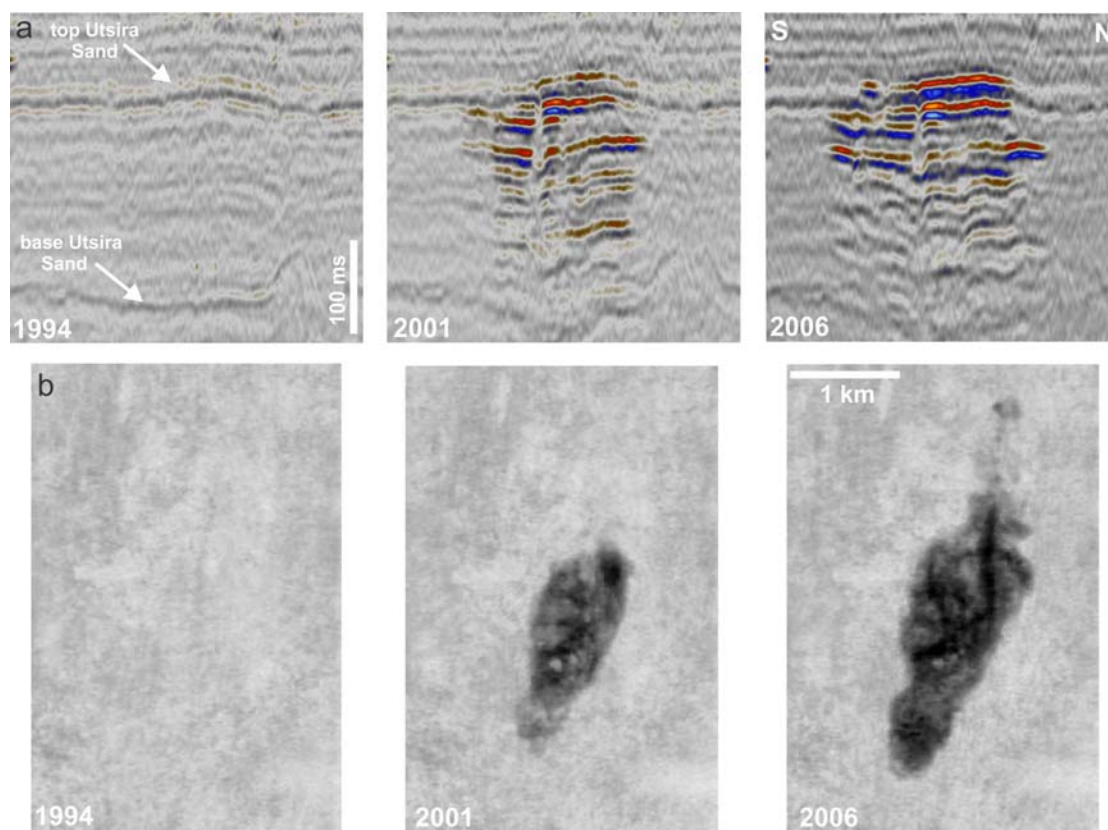


Fig. 2 Time-lapse seismic data from Sleipner showing growth of the CO₂ plume from 1994 (prior to injection) to 2006. a) N-S section through the plume with its characteristic tiered structure of reflectivity b) maps of total reflectivity within the Utsira reservoir with the characteristic elliptical plume footprint.

The plume is tiny in comparison with the estimated capacity of the Utsira reservoir. The 13 million tonnes of CO₂ injected by late 2011 had an *in situ* volume around $18 \times 10^6 \text{ m}^3$. The total pore volume of the Utsira Sand has been estimated at $6 \times 10^{11} \text{ m}^3$ (Chadwick et al. 2004b), so the percentage of the total Utsira pore-space replaced by CO₂ was around 0.003%.

3. Estimating pressure effects in the Utsira Sand from reservoir flow simulations

The potential pressure response of the Utsira Sand to the Sleipner injection was investigated via a suite of simple numerical flow models using the TOUGH2 reservoir flow simulator incorporating the ECO2N equation-of-state (Pruess 2005).

The models are axisymmetric (radial symmetry), with the injection point on the axis, and a radial element mesh. The mesh extends out to 200 km and was set up to allow the inclusion of vertical flow barriers at radii of 5 km, 10 km, 20 km and 40km, creating cylindrical pressure compartments of various sizes around the wellbore (Fig. 3).

Initial P/T conditions were set with hydrostatic fluid pressures. A salt mass fraction of 0.032 was used throughout, reasonable for a shallow saline storage aquifer. Solubility of CO₂ in saline water is also taken into account (Pruess 2005).

	Reservoir sand	Caprock/ underburden	Barrier
Permeability	$2 \times 10^{-12} \text{ m}^2$	$3 \times 10^{-19} \text{ m}^2$	$3 \times 10^{-19} \text{ m}^2$
Porosity	0.37	0.32	0.37
Capillary entry pressure	4 kPa	1 MPa	400 kPa

Table 1 Parameter values used in TOUGH2 flow models

The reservoir was set with its top at a depth of 800 m, 250 m thick and with homogeneous properties (Table 1), based on geophysical log data and a limited amount of core (Zweigel et al. 2004). The temperature at the top of the reservoir was assumed to be 29 °C and at the injection point 36 °C, consistent with the latest measurements by Statoil on water produced from the nearby Volve field. The reservoir formation was capped and underlain by 50 m thick layers both of very low permeability and high capillary entry pressure (Table 1) consistent with measured values for the caprock (Harrington et al. 2010). The modelling neglects any potential chemical reactivity of CO₂. This is in line with experimental and modelling studies (summarised in Chadwick et al. 2008), indicating that geochemical effects of CO₂, both on the reservoir sand and on the caprock, will likely be very small.

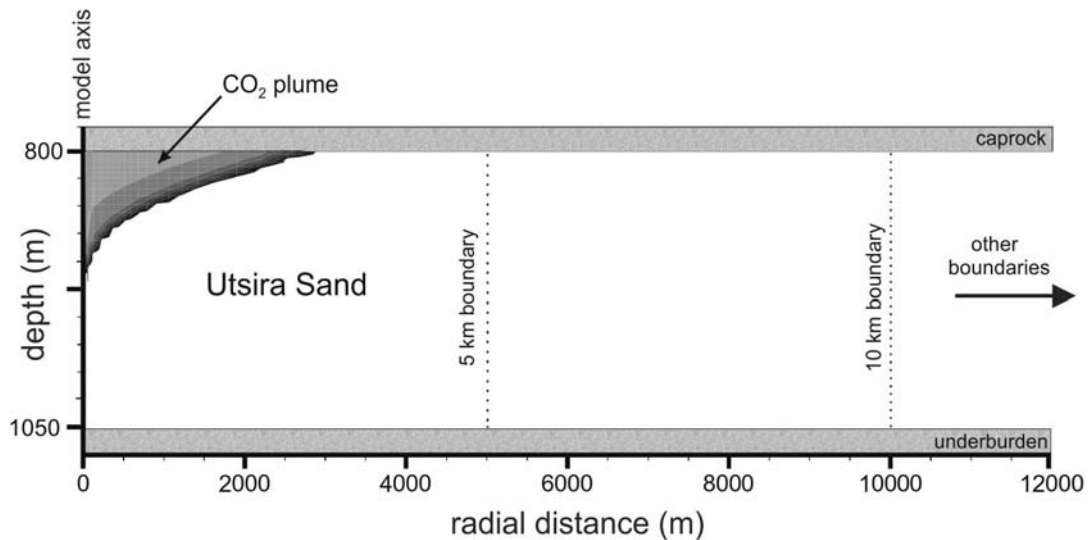


Fig. 3 Schematic diagram showing the main elements of the TOUGH axisymmetric model of the Utsira Sand. The full model extends out to a radial distance of 200 km.

CO₂ injection was simulated for 20 years at a constant rate of 28.16 kg.s⁻¹ (0.89 Mt.yr⁻¹) at a depth of 1012 m. In the model, injection was into a single mesh element of radius 5 m and a height of 2 m, whereas in reality CO₂ is injected along a 38 m

perforated horizontal length of the well. The use of the cylindrically symmetric model precludes a more realistic representation of the wellbore, but the result is that pressures in the immediate vicinity of the injection point may be expected to differ significantly between the model and the field situation. At distances greater than a few tens of metres however differences should be small.

An initial model was run with the outer boundary set at a radius of 200 km. This lies well outside the actual limit of the Utsira Sand and thus approximates to a situation where the reservoir is laterally 'open', with hydraulic connectivity to adjacent reservoir formations. The next model had its outer boundary set at 40 km. This approximates to the actual reservoir limits in the southern part of the Utsira Sand (Fig. 1) and therefore roughly represents a situation where the reservoir is laterally closed. Subsequent models were run with the outer boundary set at 20 km, 10 km and 5 km. These represent hypothetical flow barriers within the reservoir itself, giving progressively tighter pressure compartmentalisation about the injection point. Reservoir pressures were calculated for the years 2001 and 2006 (after 5 and 10 years of injection respectively), corresponding to the dates of two of the time-lapse 3D seismic surveys (see below).

The 200 km 'open aquifer' simulation shows only a small increase in pressure, ΔP decreasing from around 0.14 MPa close to the injection point to less than 0.02 MPa at 40 km (Fig. 4a). Within 5 km, a steady-state is reached and pressures do not change much between 2001 and 2006. Beyond 5 km, pressures do increase slightly as pressure propagates progressively into the far-field. The 40 km simulation (Fig. 4b) is similar to the 200 km case, around the injection point, but the effects of the reservoir boundary are evident as more rapidly increasing pressures in the far-field. The cases with progressively closer (intra-reservoir) boundaries (Figs. 4 c, d, e) show increased values of ΔP , more uniform distribution of pressure away from the injection point, and a more-or-less linear increase in pressure with time. This is most evident for the 5 km boundary simulation (Fig. 4e), where a ΔP value of 0.9 MPa in 2001 increases to ~1.7 MPa in 2006.

It is noted that away from the plume itself (where buoyancy effects due to the CO₂ layers and viscous effects around the injection point are evident), vertical pressure differences in the reservoir increase in the reservoir are extremely small, typically \ll 1% of the pressure increase.

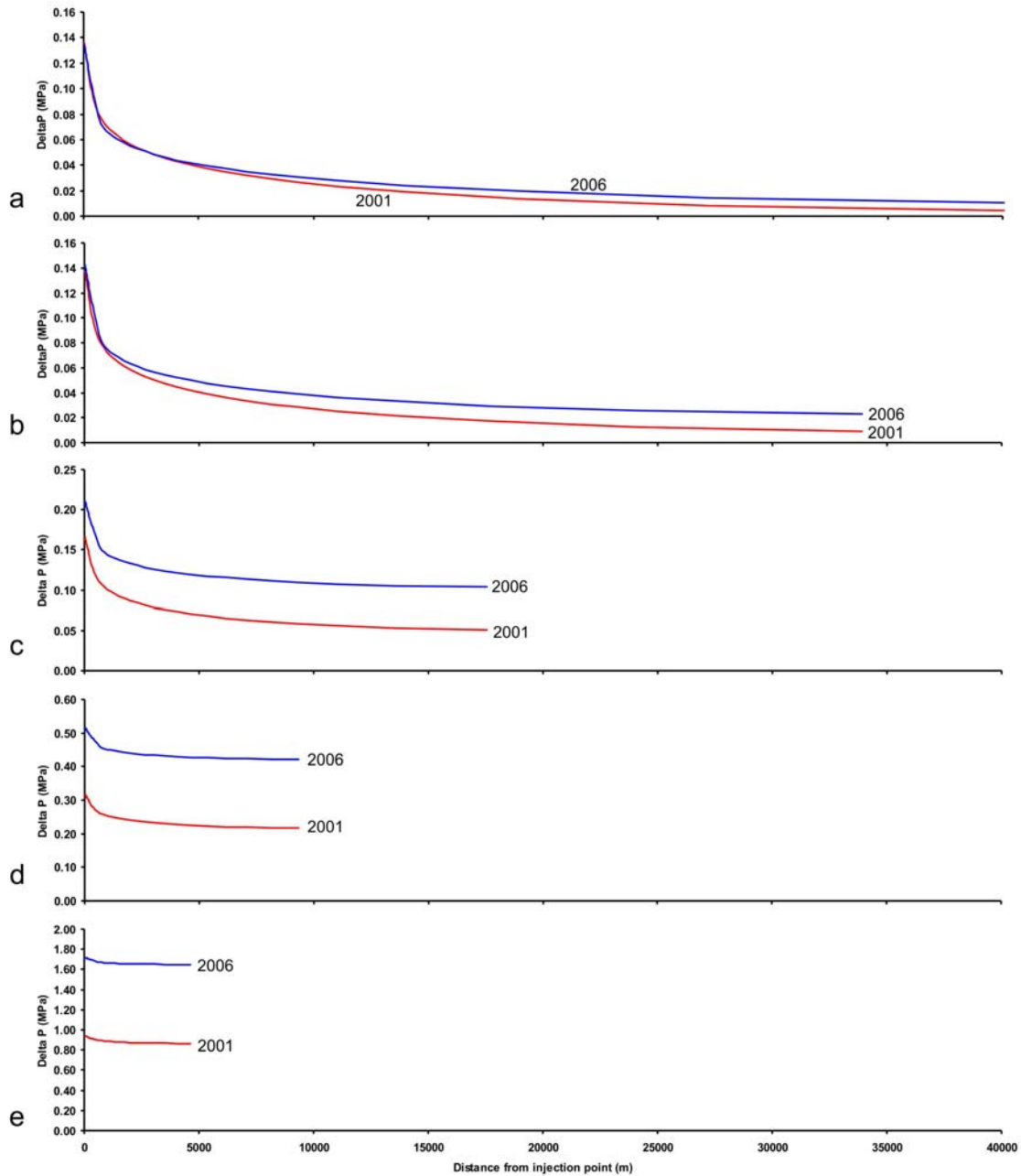


Fig. 4 Calculated pressures in 2001 and 2006 as a function of radial distance for various reservoir boundary conditions a) boundary at 200 km b) boundary at 40 km c) boundary at 20 km d) boundary at 10 km e) boundary at 5km. Note different vertical scales.

The time-lapse 3D seismic dataset covers an area of around 16.7 km², and includes 116532 individual seismic traces ranging between zero and 4.05 km from the injection point. So, focussing on the near-field pressures, i.e. within 5 km of the injection point (Fig. 5), it is clear that they are controlled by the distance of the no-model boundary in two ways. Firstly the closer boundaries show a markedly higher pressure increase (by more than an order of magnitude). Secondly the closer boundaries drive a significant increase in pressure from 2001 to 2006 (roughly a factor of two), whereas the near-field increase between 2001 and 2006 with the more distant boundaries is barely discernible.

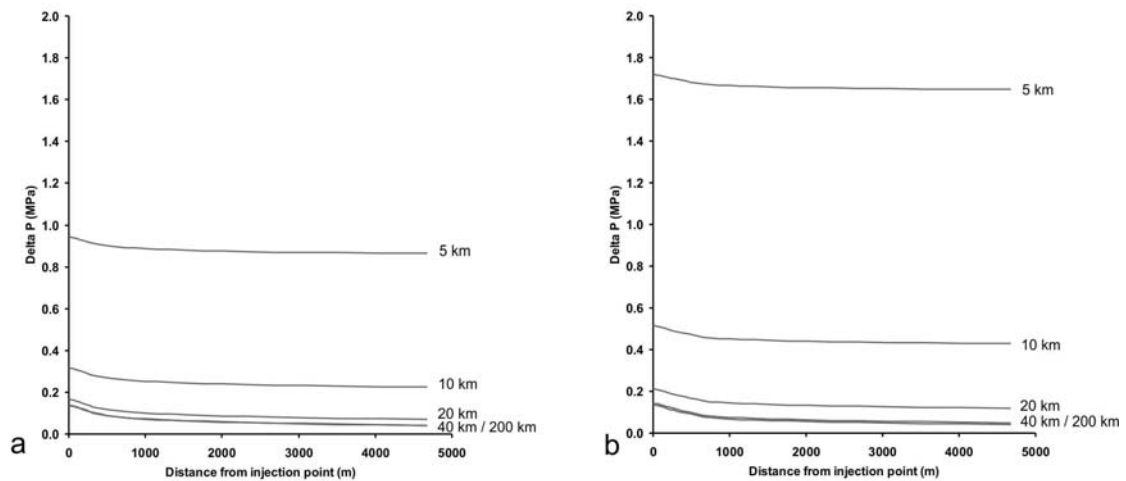


Fig. 5 Calculated pressures for the innermost 5 km of the flow model and the range of boundary conditions a) 2001 b) 2006.

In summary, the simulations indicate that an uncompartimentalised reservoir would be characterised by near-field (1 to 5 km from the injection point) pressure increases of around 0.1 MPa or less, whereas increasing degrees of compartmentalisation will lead to near-field pressure increase of 0.5 MPa or greater.

4. Pressure Monitoring data

No downhole reservoir pressure readings have been taken at Sleipner, but wellhead pressures have been measured since the start of injection in 1996 (Fig. 6).

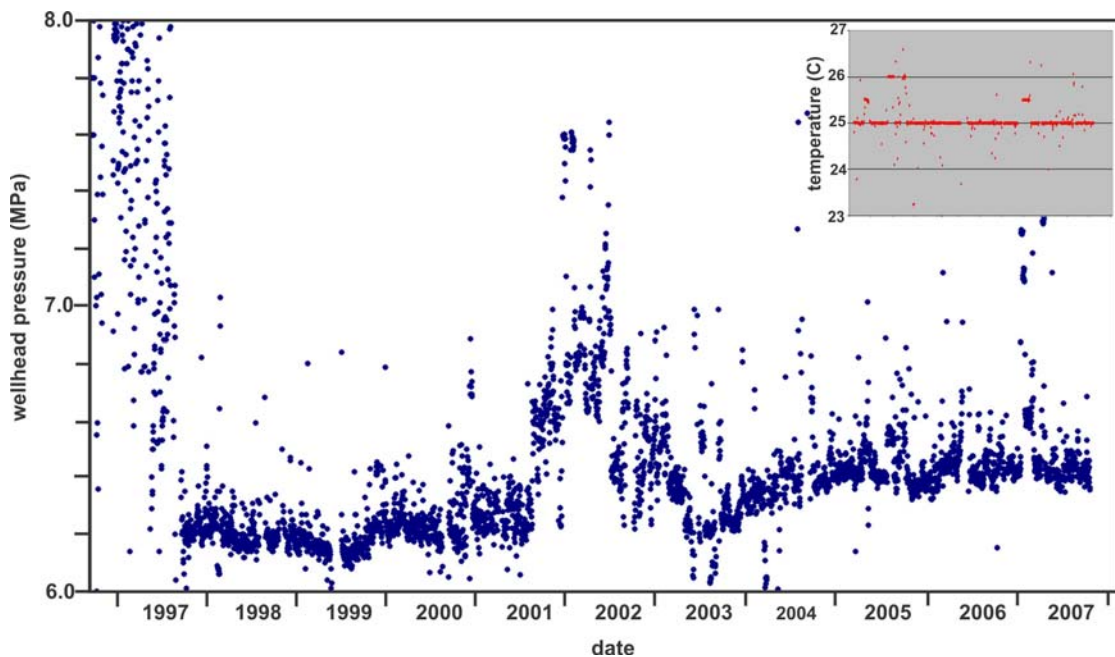


Fig. 6. Wellhead pressures and temperatures (inset), measured at Sleipner, 1996 to 2007.

Two prominent features in the measured data are irregularly high pressures for the first few months and a prominent high pressure excursion from late 2001 to early 2003. These were caused by specific technical problems related to the injection infrastructure: the former due to sand blocking the perforation screens, an issue that was subsequently remediated, and the latter due to problems with the wellhead thermostatic temperature control (see below). Setting aside these anomalous readings, the wellhead data indicate early wellhead pressures of around 6.2 MPa (1997 to 2001) with rather higher pressures of around 6.4 MPa from about 2005 onwards.

Neglecting frictional effects associated with fluid transport down the well, downhole pressure at the injection point (approximating to near-wellbore formation pressure) is a function of the wellhead pressure and the weight of the CO₂ column in the wellbore:

$$P_{IP} = P_{WH} + g \int_0^Z \rho(z) dz \quad \text{Equation 1}$$

Where:

P_{IP} = downhole pressure at the injection point (depth Z)

P_{WH} = wellhead pressure (measured)

g = acceleration due to gravity

$\rho(z)$ = density of the injected CO₂ in the wellbore at depth z

Downhole pressure therefore depends on the density of the CO₂ column in the wellbore. This varies with temperature and pressure. Early in the injection history, CO₂ temperature at the wellhead was around 23 °C (Korbøl and Kaddour 1995), but from early 2005, measurements show accurate thermostatic control at 25 °C (Fig. 6), and uniform wellhead pressures. In fact it is not straightforward to calculate reservoir pressure from wellhead pressure as the temperature profile in the wellbore is not accurately known. In addition, the CO₂ in the wellbore lies close to the dewpoint, so (boiling) fluid and (condensing) vapour phases of markedly different densities can interchange with small P,T variation (Alnes et al. 2011). Because of this, downhole pressure does not necessarily have a simple offset from wellhead pressure. Circumstantially, the uniform pressures which correspond to the close thermostatic control from 2005 onwards are consistent with negligible pressure increase in the reservoir but this cannot be proven.

5. Seismic monitoring for pressure changes

Seismic data provide a powerful means of identifying changes in the reservoir fluids both in terms of their composition and their pressures. The seismic response to the fluid substitution effects of CO₂ replacing formation brine in the Sleipner plume is clear (Fig. 2) and has been well described in the literature (e.g. Chadwick et al. 2005, Arts et al. 2008). In contrast, the seismic response to changes in reservoir pressure has not previously been examined in detail.

The main effect of fluid pressure increase in a reservoir is to reduce the strength of the rock matrix by reducing the normal and shear-stresses at the grain-to-grain contacts in the reservoir rock (Fig. 7). This in turn reduces the bulk and shear moduli of the rock which determine its seismic velocity.

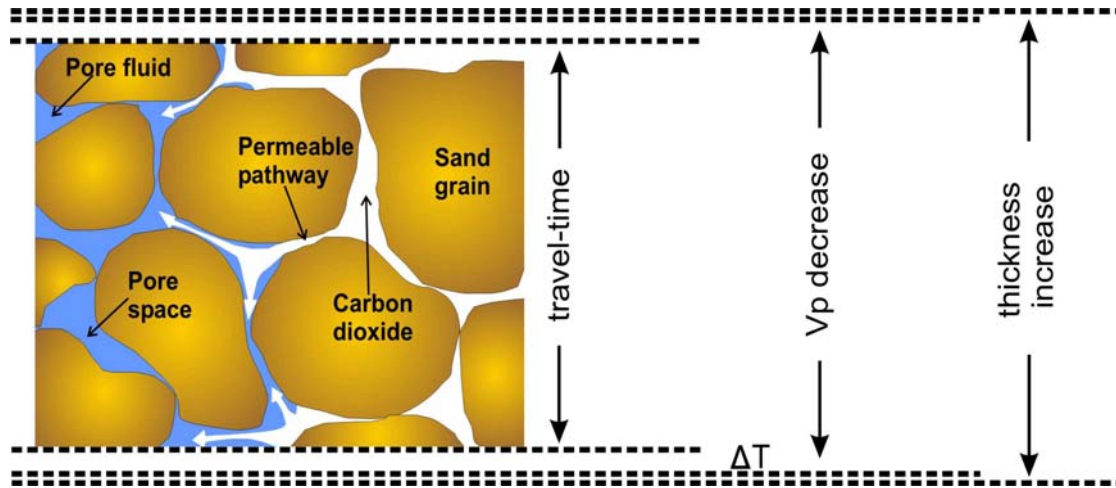


Fig. 7. Schematic diagram of CO₂ replacing brine in a porous sand. Pressure increase reduces seismic velocity V_p and increases travel-time across the formation. A minor increase in reservoir thickness may also occur.

A secondary effect is to induce a minor geomechanical ‘inflation’ of the reservoir itself, producing a real increase in reservoir thickness (Fig. 7). This has been observed at the In Salah CO₂ storage site in Algeria (e.g. Onuma and Ohkawa 2008). Both the seismic and the geomechanical effects act in the same sense: to produce an increase in seismic travel-time from the top to the base of the reservoir.

In principle therefore, if we avoid the saturation footprint of the CO₂ plume itself, accurate measurements of two-way travel-time changes (‘time-shifts’) across the Utsira Sand should provide a measure of changes in reservoir pressure.

5.1 Dependence of V_p and V_s on pressure

The dependence of seismic properties on pressure has been established for a range of rock types by a number of laboratory studies of elastic wave velocity in samples with varying pore-pressures (e.g. Wyllie et al. 1958; Han et al. 1986; Eberhart-Phillips et al. 1989; Zhang and Bentley 1999, Xue and Ohsumi 2004). In general, for rocks subjected to a given confining stress, higher pore-fluid pressures lower the effective stress and produce lower seismic velocities. Eberhart-Phillips et al. (1989) developed the following empirical relationships for sandstones subject to variable effective stress:

$$V_p = 5.77 - 6.94\phi - 1.73\sqrt{C} + 0.446(P_e - e^{-16.7P_e})$$

$$V_s = 3.70 - 4.94\phi - 1.57\sqrt{C} + 0.361(P_e - e^{-16.7P_e})$$

Equations 2 and 3

Where:

V_p is the p-wave velocity (kms^{-1})

V_s is the s-wave velocity (kms^{-1})

ϕ is the porosity

C is the mineral fraction of clay in the reservoir rock

P_e is the effective pressure (lithostatic pressure minus pore pressure) (kbar)

This type of relationship is likely to be particularly applicable to a sandstone that is on a normal burial trend, and hasn't suffered unusual diagenesis. The Utsira Sand fulfils these criteria admirably. The actual degree to which Equations 2 and 3 are applicable specifically to the Utsira Sand can be tested by comparing calculated values of V_p and V_s , based on measured reservoir petrophysical properties, with measured values of V_p and V_s .

Observed values of V_p for the Utsira Sand, as determined from well logs around Sleipner, range between about 2013 and 2057 ms^{-1} , with a mean value of 2036 ms^{-1} . An average value of V_s from a single shear-velocity log is 643 ms^{-1} .

Prior to CO_2 injection, the Utsira Sand is assumed to have been hydrostatic with fluid densities around 1025 kgm^{-3} (Harrington et al. 2010). Pore pressures are therefore typically in the range 8.4 MPa (at 820 m corresponding roughly to the reservoir top around Sleipner) to 10.8 MPa (at 1050 m corresponding roughly to the reservoir base). The mean depth of the reservoir within the Sleipner 3D seismic area (Fig. 2) is 937 m, giving a mean pore pressure of 9.6 MPa, a mean lithostatic pressure of 17.1 MPa (assuming an average overburden density of 1.90) and a mean effective pressure of 7.5 MPa. The more reliable measurements of porosity are in the range 0.35 to 0.42 with a mean of 0.38 and the bulk clay fraction of the formation, including the intra-reservoir mudstones, is around 0.15 (Zweigel et al. 2004).

Inserting these values into Equations 2 and 3 gives calculated values for V_p and V_s of 2286 ms^{-1} and 1078 ms^{-1} respectively. These calculated values are very sensitive to reservoir parameters however. A minor modification of properties, taking an average porosity of 0.4 and a clay fraction of 0.25, reduces calculated values of V_p to a much better match of 2035 ms^{-1} and V_s to 884 ms^{-1} . Reducing the effective pressure, which is dependent on the rather poorly-constrained overburden densities and the assumed hydrostatic conditions, would further reduce calculated velocities.

Taking into account the known parameter uncertainty, for V_p there is an acceptable match between the calculated and measured values. For V_s the match is less good, albeit based on just a single measured downhole log. For this study, we are only

interested in V_p , and, more specifically, changes in V_p rather than absolute values. It is therefore considered that Equation 2 is fit for our purpose.

Using the modified properties outlined above, V_p can be calculated for a range of reservoir pore pressure changes (Fig. 8a), with pressure increases in the range 0 – 2 MPa (0 – 20 bars) reducing V_p by up to $\sim 60 \text{ ms}^{-1}$. This rate of velocity change with pressure ($\sim 30 \text{ ms}^{-1}$ per MPa) is consistent with experimental values given by Zhang and Bentley (1999) where sandstones at effective stresses of 5 – 10 MPa showed V_p decreases between ~ 25 and $\sim 40 \text{ ms}^{-1}$ per MPa increase in pore pressure and also with values quoted in Zimmer et al. (2002) who compiled data from unconsolidated sands.

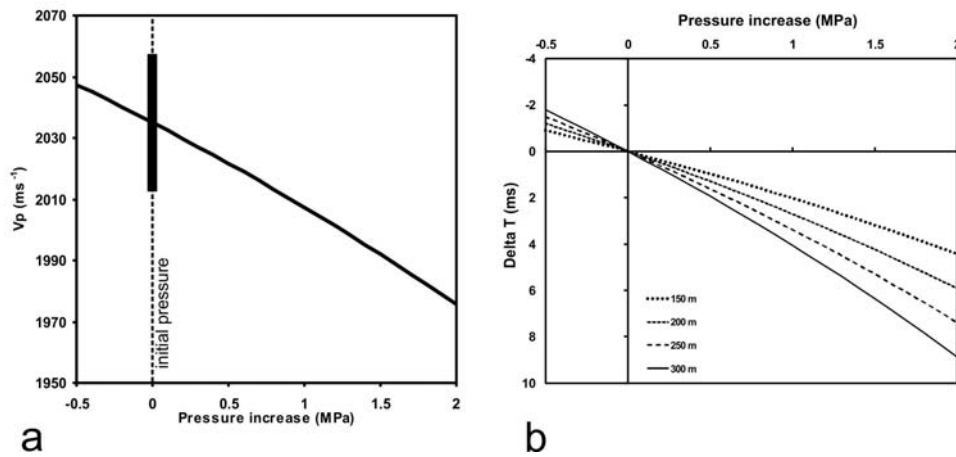


Fig. 8 a) V_p calculated from Equation 2 as a function of pore pressure increase. Bold black bar denotes range of observed V_p for the Utsira Sand around Sleipner b) Increase in travel-time (ΔT) through the Utsira Sand as a function of pore-pressure increase for a range of reservoir thicknesses (150 – 300 m).

Velocity changes of this order would produce a significant increase in the seismic two-way travel-time through a thick reservoir such as the Utsira Sand. Around Sleipner, the reservoir varies from around 150 m to 300 m thick (Fig. 1a). With a measured average V_p around Sleipner of 2036 ms^{-1} , two-way travel-times through the Utsira Sand are correspondingly in the range 150 to 300 ms (Fig. 2). Travel-time changes scale directly with velocity change and with reservoir thickness, so it is straightforward to calculate travel-time changes as a function of pressure increase and reservoir thickness (Fig. 8b). A pressure increase of, for example, 2 MPa would therefore produce a travel-time increase of around 4 ms in the thinner parts of the reservoir and over 8 ms where it is thickest.

5.2 Changes in reservoir thickness with pressure

In addition to changing the seismic velocity, an increase in fluid pressure will induce a small geomechanical increase in reservoir volume:

$$\Delta V = \beta_p \bar{V} \Delta P \quad \text{Equation 4}$$

Where:

ΔV is the change in reservoir volume

V is the initial total reservoir volume
 \emptyset is the reservoir porosity
 ΔP is the increase in pore-pressure
 β_p is the pore compressibility

A hypothetical cube of rock within the reservoir, and with isotropic *in situ* confining stress, would expand equally in all directions as pore-pressure increases. Thus:

$$\Delta T \approx (\beta_p \emptyset T \Delta P) / 3 \quad \text{Equation 5}$$

Where:

ΔT is the change in reservoir thickness
 T is the initial reservoir thickness

For the Utsira Sand around Sleipner we can take a mean reservoir thickness of 200 m and a mean porosity of 0.38. Pore-compressibility is not a well-constrained parameter, but here we take a value of $4.5 \times 10^{-10} \text{ Pa}^{-1}$ which is typical of poorly-consolidated rocks such as the Utsira Sand (Freeze and Cherry 1979). Substituting these values into Equation 5, a pressure increase of 2 MPa (20 bars) will induce a thickness change of around 0.02 metres. Given a mean Vp of 2050 ms^{-1} for the Utsira Sand, such a thickness change would cause a two-way travel-time increase of around 0.02 ms.

In reality *in situ* stresses are unlikely to be perfectly isotropic. Wiprut & Zoback (2002) state that a strike-slip stress regime is typical of the northern North Sea, with the vertical (overburden) stress intermediate between the two horizontal stresses. In terms of thickness changes, this situation does not differ strongly from the isotropic stress situation. Irrespective of the stress field details, the thickness change is more than two orders of magnitude smaller than the predicted travel-time changes caused by the velocity effect, and so, for the purposes of this analysis is neglected (it is worth noting that geomechanical effects would in any case enhance the seismic effect by increasing travel-times through the reservoir).

5.3 Travel-time changes through the Utsira Sand

A comprehensive time-lapse surface seismic programme has been carried out at Sleipner, including 3D surveys in 1994 (two years prior to start of injection), 1999, 2001, 2002, 2004, 2006 and 2008. The 3D datasets covered a rectangular area centred over the plume, measuring some 5.8 km by 3.1 km (Fig. 2) with a total of 116532 individual seismic traces.

The time-lapse 3D seismic data provide an ideal tool with which to measure travel-time changes (time-shifts') through the Utsira Sand. In order to maximise accuracy we have taken three surveys from the 2006 time-lapse processing ensemble: 1994 (baseline), 2001 and 2006. These have been subject to the same parallel processing sequence with careful matching between the surveys to minimise any mismatches in reflectivity and travel time arising from non-perfect repeatability of the surveys.

There are three key seismic picks for the analysis (Fig. 9): the top of the Utsira Sand, the top of the 5-metre mudstone (a bright coherent reflector closely beneath the top Utsira) and the base of the Utsira Sand. The seismic picks were made using 2D autopicking (to ensure accurate ‘lock-on’ to the peak or trough) on the 1994, 2001 and 2006 surveys. An example of the picking shows generally good repeatability between the surveys (Figs. 9 a, b).

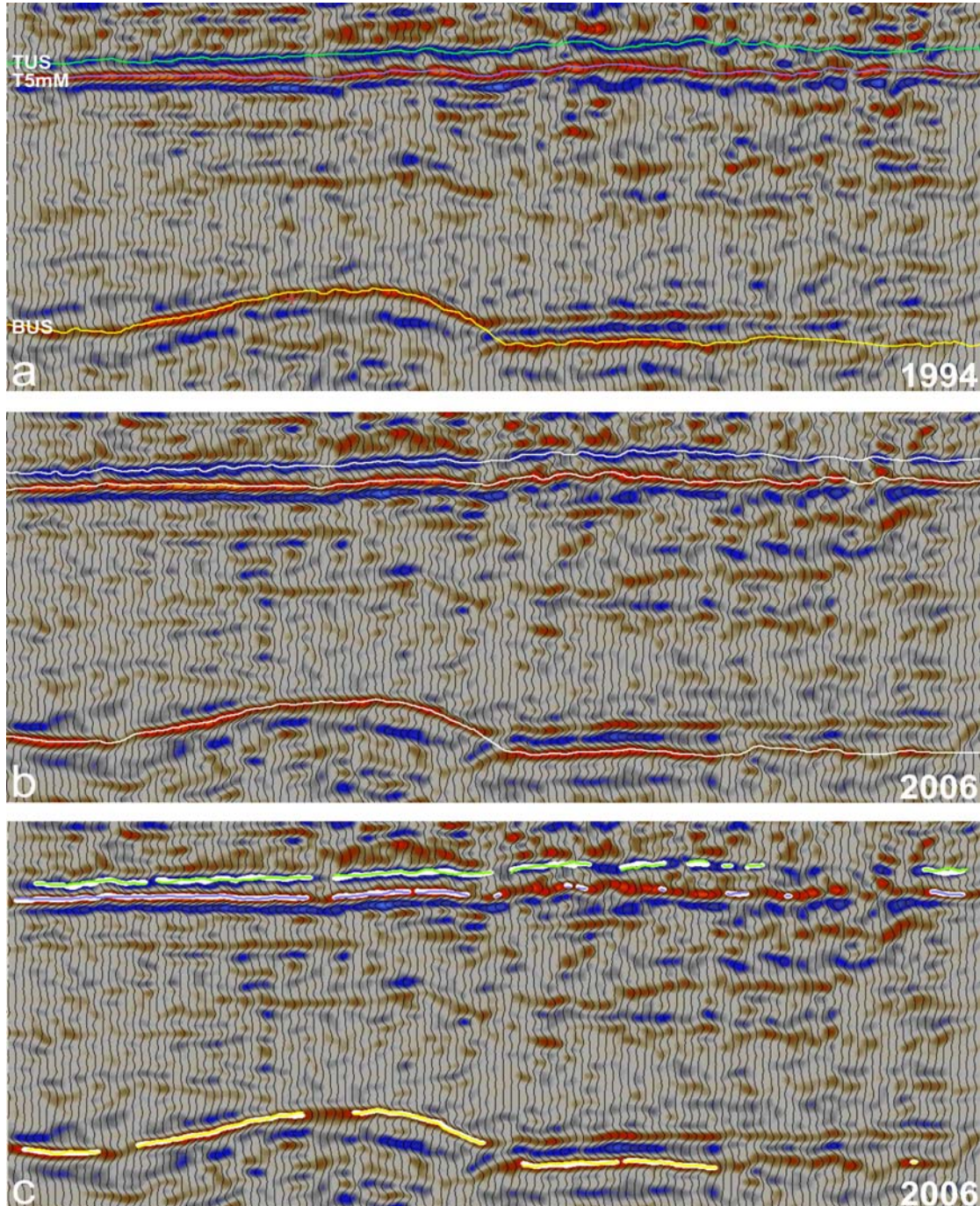


Fig. 9. a) East - west crossline from the time-lapse 3D datasets, outside of the CO₂ plume footprint. a) 1994 data with 1994 seismic picks b) 2006 data with 2006 seismic picks c) 2006 data showing decimated 2006 picks (in bold white) and superimposed decimated 1994 picks (in colour). TUS = Top Utsira Sand, T5mM = Top 5metre mudstone, BUS = Base Utsira Sand.

By subtracting the top and base Utsira picks, travel-time changes through the Utsira Sand can readily be measured (Fig. 10). The strong velocity pushdown effect of the CO₂ plume is clear, with systematic increases in travel-time of up to 50ms corresponding to the footprint of the reflective plume. This is largely a consequence of substituting CO₂ for water within the plume. Outside of the plume footprint, real travel-time changes cannot be due to free CO₂, but pressure effects, which are transmitted readily through the reservoir pore-water (see above), could potentially be detectable. It is clear that outside the plume footprint, time-shifts are very much smaller, but with scattered peaks showing both negative and positive changes (typically up to +/- 10 ms). These correspond to areas where there is a degree of mismatch between the picks on the baseline and repeat survey, particularly where there is pick uncertainty in areas of poorer data quality.

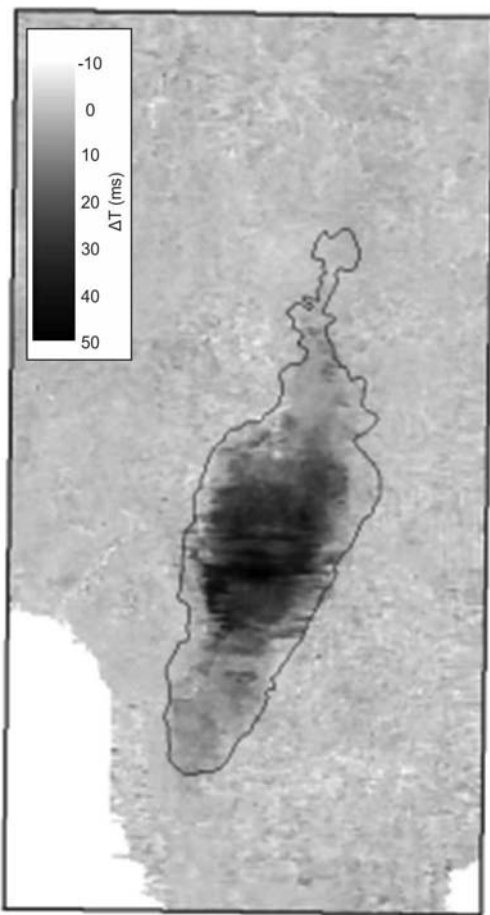


Fig. 10. Travel-time changes through the Utsira Sand between 1994 (prior to injection) and 2006. Note the very strong velocity pushdown effect beneath the CO₂ plume, due to fluid substitution effects. In the southwestern and far southeastern extremities of the 3D dataset it is not possible to make reliable picks of the top and base of the reservoir. Black polygon denotes the reflectivity footprint of the plume in 2006.

In order to accurately measure any travel-time changes caused by pressure increase, it is necessary to consider only those traces which lie outside of the area of the plume footprint to exclude the (very large) effects of fluid substitution. It is also evident that

in some areas the picks are much less clear and coherent than others, and measured changes in travel-time will be correspondingly inaccurate. In order to address this, the picks were decimated to include only areas where the seismic events show high amplitude and coherency, where the autopicking algorithm gave good reliability (Fig. 9c). It can be seen from the superimposed picks in these high coherency areas that two-way travel-times are very similar on successive surveys, but still with trace-to-trace time-lapse variations or ‘jitter’ of a few milliseconds.

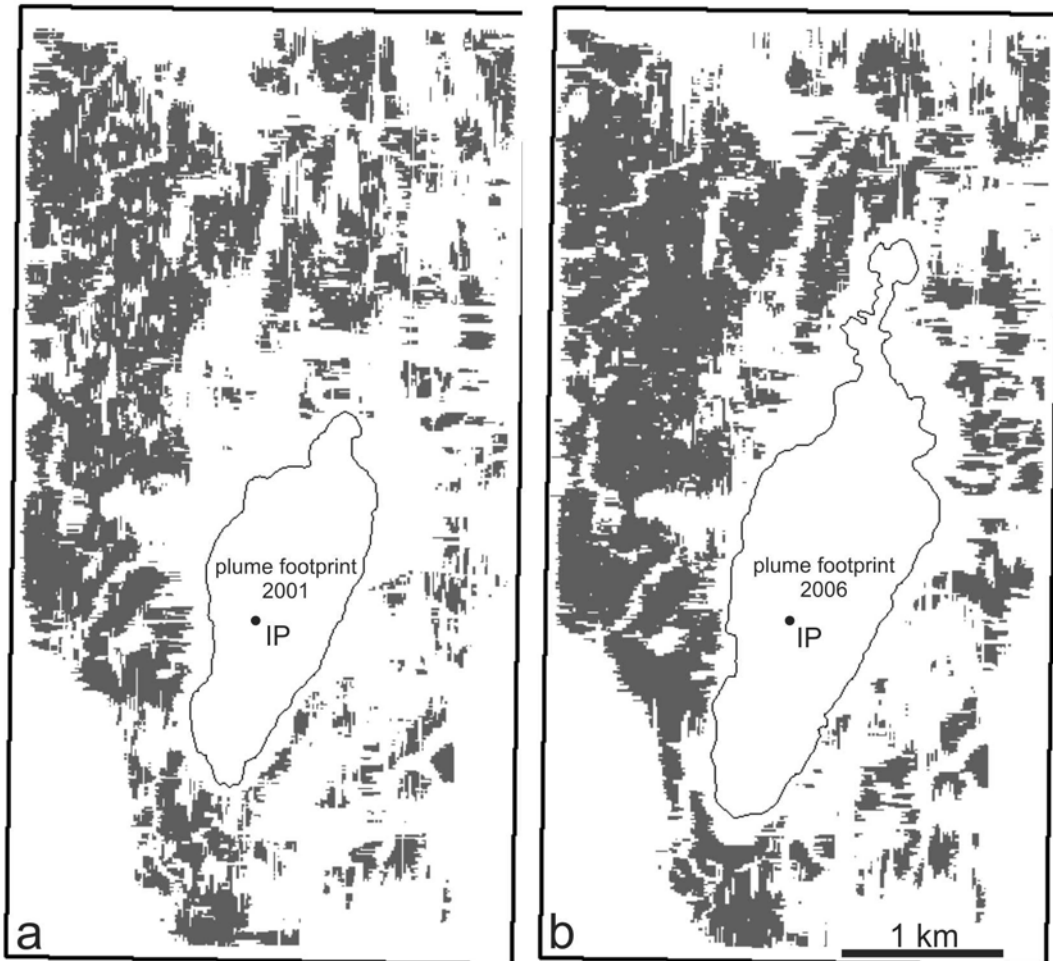


Fig. 11 Decimated (high quality) traces (in grey) utilised in the Utsira (TUS-BUS) travel-time analysis for a) 2001 survey b) 2006 survey. IP = injection point.

Eliminating areas where either the top or base reservoir picks were of insufficient quality results in a somewhat patchy coverage outside of the plume footprint (Fig. 11), but with reasonably representative spatial sampling. In fact the high quality picks make up about 30 - 35 % of the total area outside of the plume footprint and comprise over 30000 seismic traces. It is notable that the decimated dataset does not sample close to the injection point, due to the necessity of avoiding the CO₂ plume footprint. Typical distances are in the range 1 to 4 km from the injection point, where the predicted pressure field is rather uniform and smoothly varying (Fig. 5).

Time-lapse changes in travel - time through the Utsira Sand were captured from the decimated seismic picks i.e. outside of the plume footprints, and also where both top Utsira (TUS) and base Utsira (BUS) picks can be made on high quality events. Time-

shifts for the periods 1996 to 2001 and 1996 to 2006 are plotted on Figs 12a and 12c respectively.

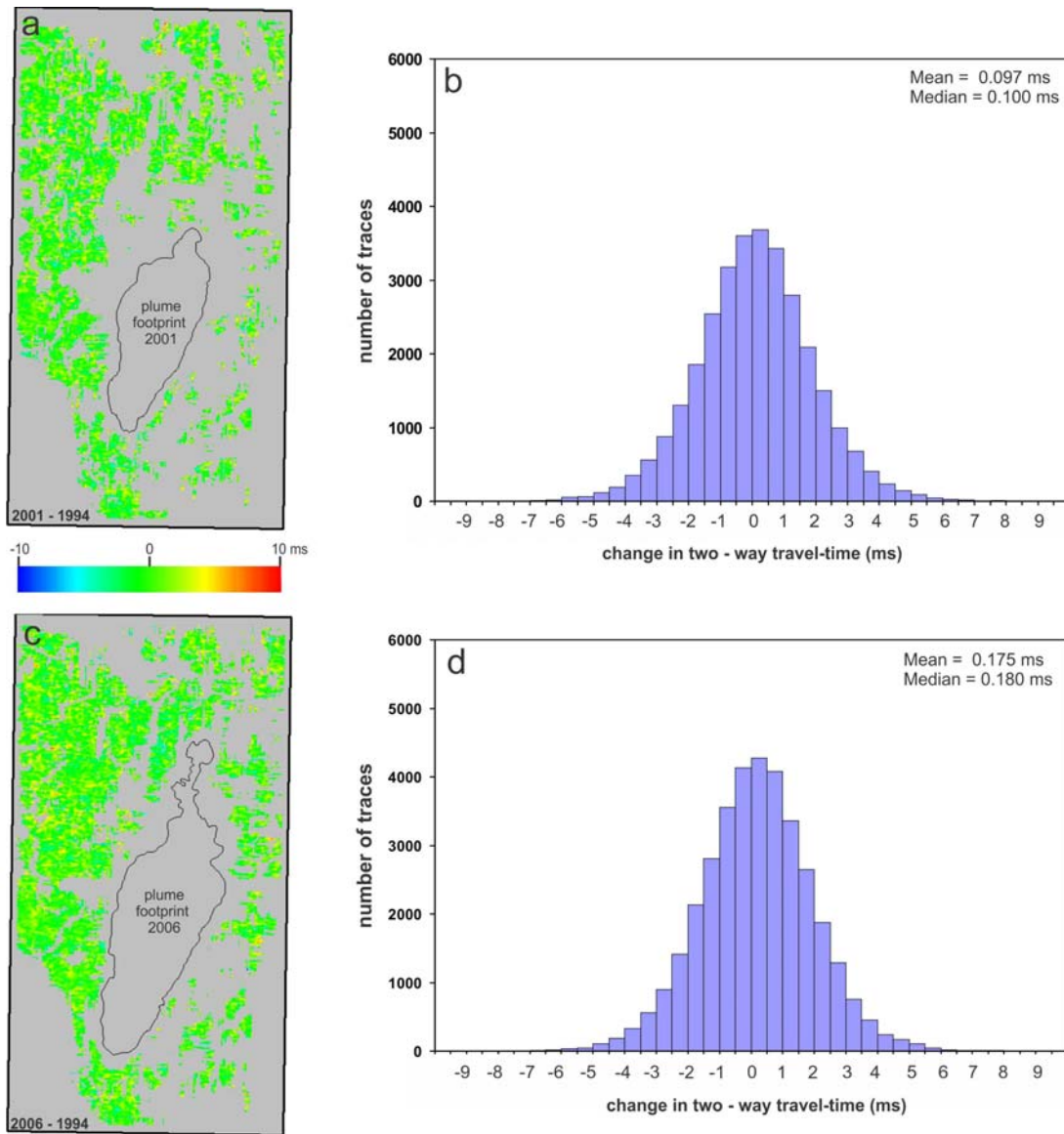


Fig. 12. ΔT maps and histograms for the TUS-BUS decimated dataset a) Mapped changes from 1994 to 2001 b) Histogram of changes 1996 to 2001 c) Mapped changes from 1994 to 2006 d) Histogram of changes 1996 to 2006.

At this point it is important to assess the potential travel-time resolution obtainable with this procedure. The field sampling rate of the 3D seismic datasets at Sleipner is 2 ms, which means that the waveforms at the top and base Utsira (with dominant frequencies typically around 40 Hz) are fully Nyquist sampled and can be reconstructed accurately by interpolation. Actual sample rates in the interpolated waveforms depend on the dynamic range of the data and the rate of amplitude change with time, but for these datasets is typically around 0.5 ms at the wavelet peaks and

troughs. For a single trace therefore the effective discrimination limit on travel-time will be around 0.5 ms. For a large number of traces, such as we have here, statistical considerations mean it is probably significantly less than this (see below).

The mapped time-shifts (Figs 12 a, c) are similar for both 2001 and 2006 with no clear systematic spatial variation. Time-shift values are of the order of a very few ms, with scatter peaks significantly smaller than on the undecimated dataset (Fig. 10). The scatter exists because the data are not noise free: the picked events at top and base reservoir show small trace-to-trace travel-time mismatches or ‘jitter’ between successive repeat surveys. This ‘jitter’, due to non-perfect repeatability of the time-lapse surveys, has a high spatial frequency and is likely to be essentially random. In contrast, any systematic changes in travel-time between time-lapse surveys will probably be very similar at top and base reservoir so will be cancelled out in this analysis. By looking at travel-time differences through the reservoir, we see only the random travel-time ‘jitter’.

Histogram plots of the time-shifts show near-symmetrical distributions (Figs 12 b, d) and in doing so provide a powerful statistical tool for determining the true average value of travel-time change. For the period 1996 to 2001 the mean travel-time change was 0.097ms, increasing to 0.175 ms by 2006. Median values are similar.

The same analysis was also applied to travel-time differences between the Top 5 metre mudstone (T5mM) and the Base Utsira picks, which spans around 90 % of the full Utsira Sand thickness (Fig. 9). This has the significant advantage that the T5mM pick tends to be rather more coherent and repeatable than the Top Utsira pick over most of the area. The T5mM – BUS decimated dataset has an overall spatial coverage similar to the TUS- BUS dataset. The T5mM-BUS histograms (Figs 13b, d) still show the markedly symmetrical distribution, but are somewhat ‘tighter’, with smaller spread, reflecting the improved signal quality. For the period 1996 to 2001 the mean travel-time change was 0.133ms, increasing to 0.158 ms by 2006. Median values are similar.

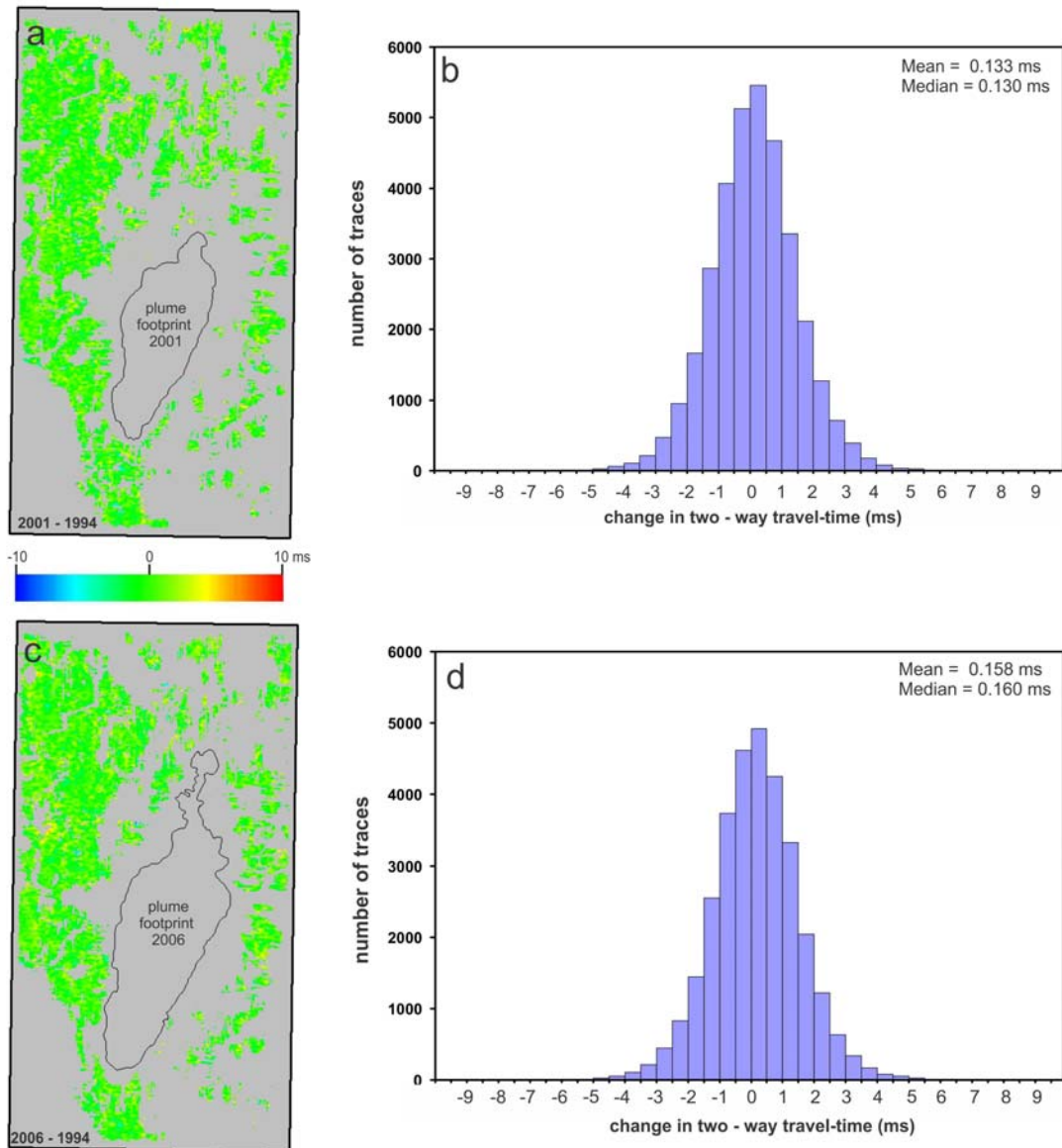


Fig. 13. ΔT maps and histograms for the T5mM-BUS decimated dataset a) Mapped changes from 1996 to 2001 b) Histogram of changes 1996 to 2001 c) Mapped changes from 1996 to 2006 d) Histogram of changes 1996 to 2006.

Both TUS-BUS and T5mM-BUS datasets show mean and median travel-time changes of less than 0.2 ms, the largest mean travel-time change of 0.175 ms being seen on the 1996 – 2006 TUS-BUS dataset. The mean Utsira reservoir thickness over the area of the 3D seismic is 235 m. ΔT values corresponding to pressure changes in the range 0.1 MPa to 1 MPa can be calculated for a reservoir of this thickness from the curves in Fig. 8b and the TUS-BUS travel-time distribution can be compared with these calculated values (Fig. 14). It is clear that under the assumption of a single average reservoir thickness, the observed travel-time distribution with a mean value of 0.175 ms, is not consistent with pressure changes in the range 0.5 to 1.0 MPa or higher, but rather points to a pressure change of 0.1 MPa or less (Fig. 14).

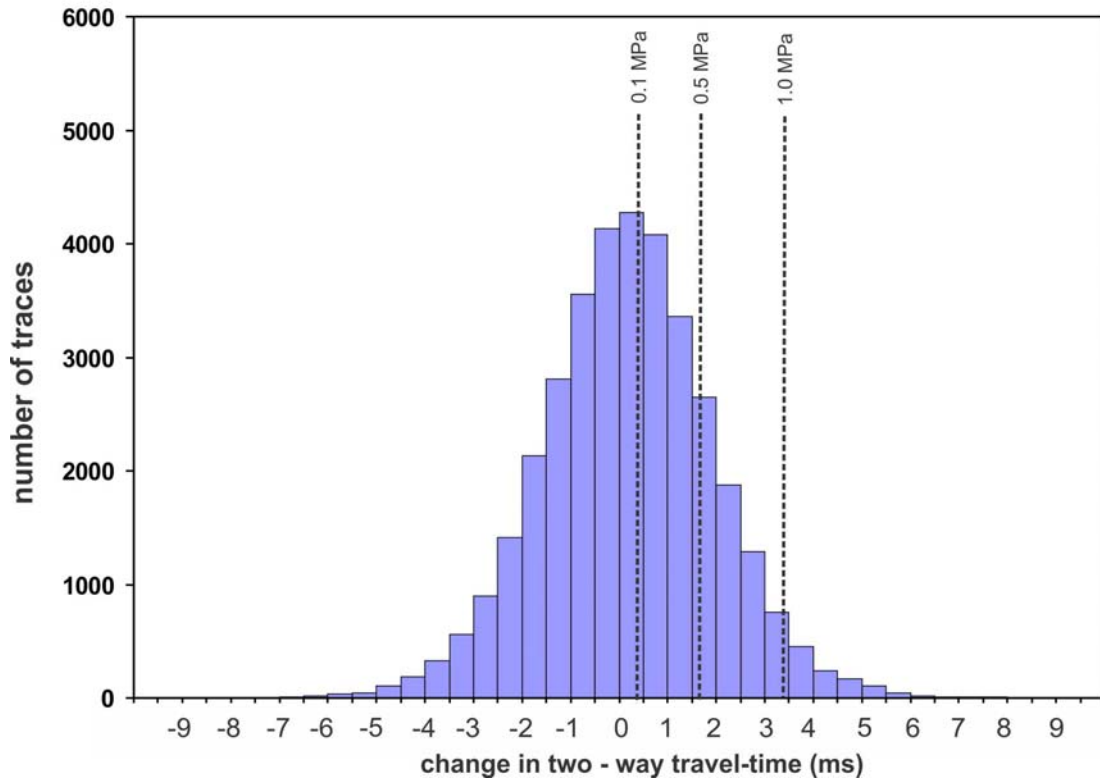


Fig. 14. Histogram of observed ΔT values for the TUS - BUS decimated dataset 1996 to 2006, compared to calculated ΔT values, for a reservoir of uniform thickness 235 m and pressure increases of 0.1, 0.5 and 1 MPa.

In terms of changes through time, the TUS-BUS datasets do show some evidence of increasing time-shifts from 2001 to 2006 (Fig. 12), perhaps suggestive of ongoing, albeit very small, pressure increase. This trend is also evident on the better constrained T5mM-BUS data, but to a significantly smaller degree (Fig. 13).

5.3.1 Statistical analysis

A more robust assessment of the pressure response of the Utsira reservoir needs to take account of known thickness variation in the reservoir, how this would affect predicted time-shifts and also how these would in turn be affected by the repeatability noise (jitter).

The T5mM-BUS dataset has the lowest travel-time scatter and is utilised for the purposes of this more robust analysis (average T5mM – BUS thickness across the dataset is 228 m). Fitting a Gaussian distribution to the T5mM – BUS 1996 to 2006 dataset (Fig. 15) shows the near normal distribution and confirms the essentially random nature of the travel-time ‘jitter’.

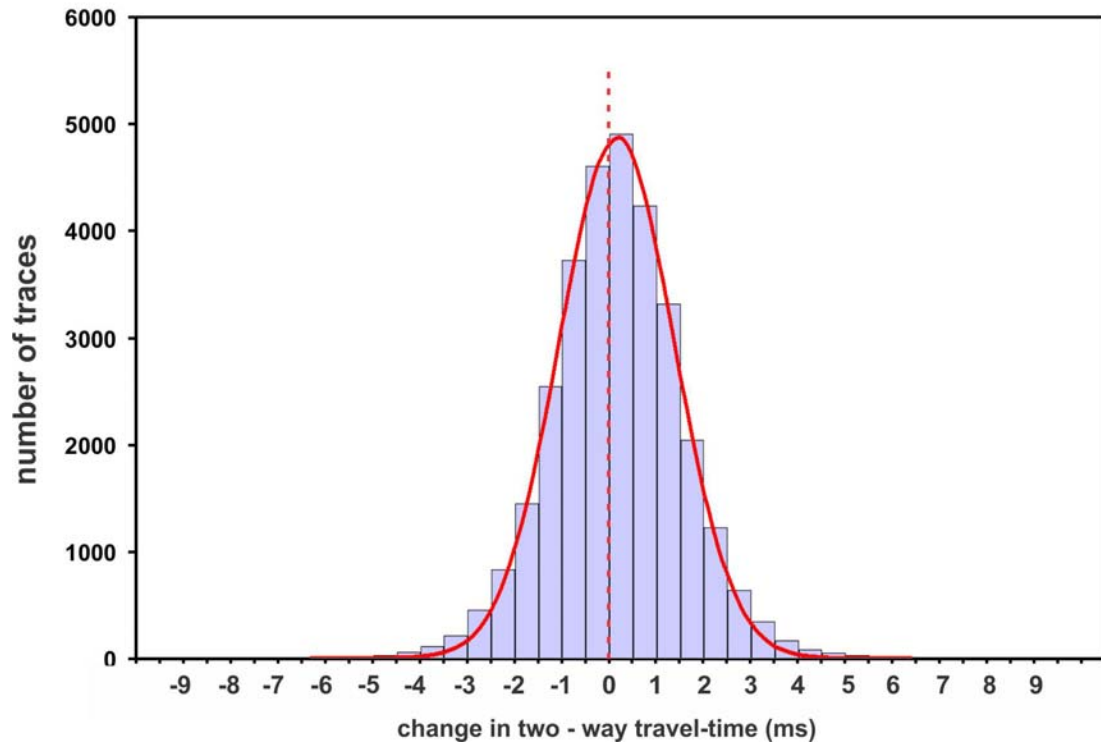


Fig. 15. Gaussian curve fitted to observed ΔT values for the T5mM-BUS decimated dataset 1996 to 2006. Note the small positive shift compared to the zero line (dotted), consistent with a very small pressure increase.

The hypothetical noise-free time-shift (ΔT) response of the reservoir scales directly with reservoir thickness and can be calculated for a given pressure increase from the relationship in Fig. 8b. Thicknesses from T5mM to BUS vary in the study area from around 150 to 300 m (Fig. 16a), so noise-free time-shift values would range from about 2 ms in the thinner parts of the reservoir to about 4 ms in the thickest. The full distributions of ΔT across the study area, for nominal pressure increases of 0.1, 0.5 and 1 MPa are illustrated in Figs. 16b, c. Thus, a nominal pressure increase of 1 MPa gives a total time-shift spread of around 2 ms (Figs 16b, c), centred on an average value of around 3.4 ms (cf Fig. 14b). Pressure increases of 0.5 MPa and 0.1 MPa give progressively smaller average values and spreads.

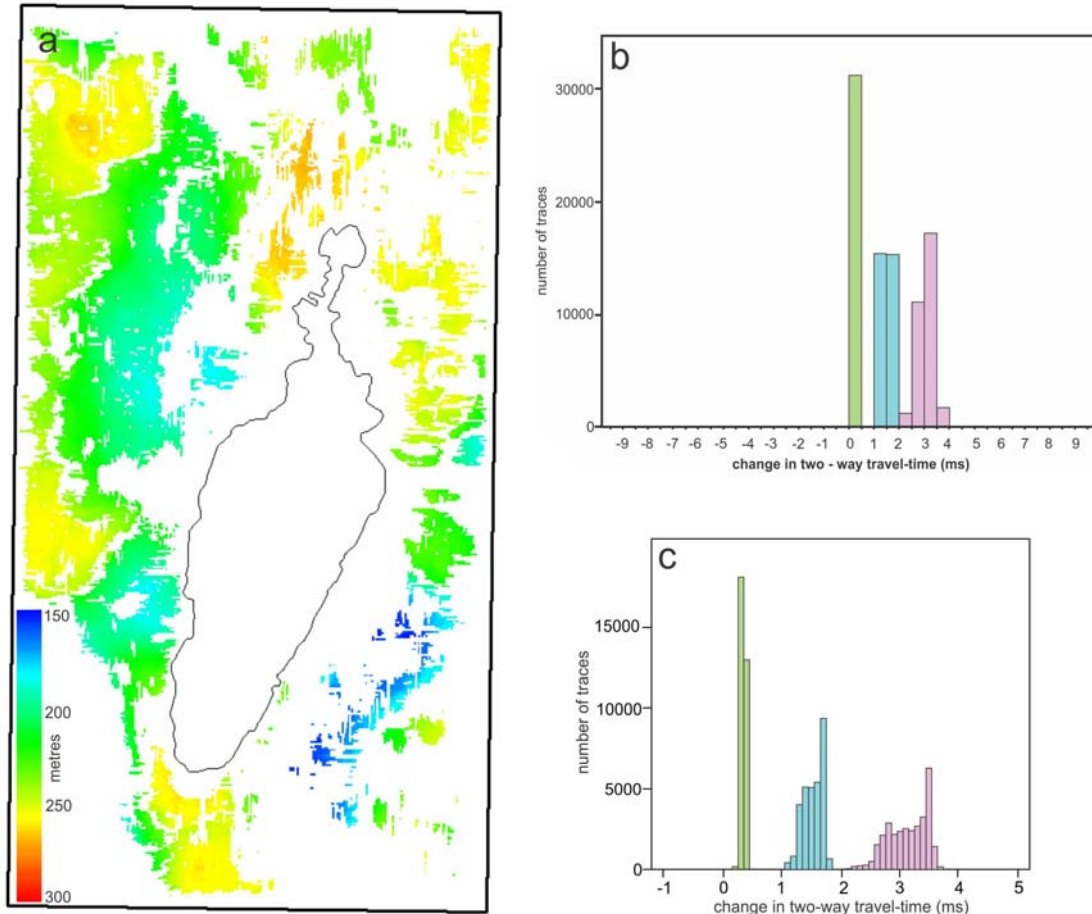


Fig. 16 a) Thickness map of the Utsira reservoir for the T5mM-BUS decimated dataset b) calculated noise-free time-shifts for this thickness distribution for pressure increases of 0.1 MPa (green), 0.5 MPa (blue) and 1 MPa (pink) c) as for b) but with the binning interval reduced to 0.1ms to illustrate the timeshift spreads more clearly.

These distributions represent the hypothetical noise-free pressure response of the aquifer - in other words, what we would see if the seismic data were perfectly repeatable with no travel-time 'jitter'. The repeatability 'jitter' imposes a much larger spread on the observed time-shift distributions. The observed distribution can therefore be expressed as the convolution of the noise-free response with the repeatability noise:

$$R_{\text{obs}} = R_{\text{noise-free}} * N_{\text{repeat}} \quad \text{Equation 6}$$

Where:

R_{obs} = observed reservoir response

$R_{\text{noise-free}}$ = hypothetical noise-free reservoir response

N_{repeat} = repeatability noise

An estimation of the repeatability noise N_{repeat} can be obtained by comparing travel-times from a single horizon for different vintages at the top of the reservoir where time-shifts will, in principle, be due only to repeatability mismatches. Repeatability noise for the Top Utsira Sand pick (TUS) between 1994 and 2006 is plotted in Fig.

17. This is again symmetrical with a scatter range similar to the distribution for the whole Utsira Sand.

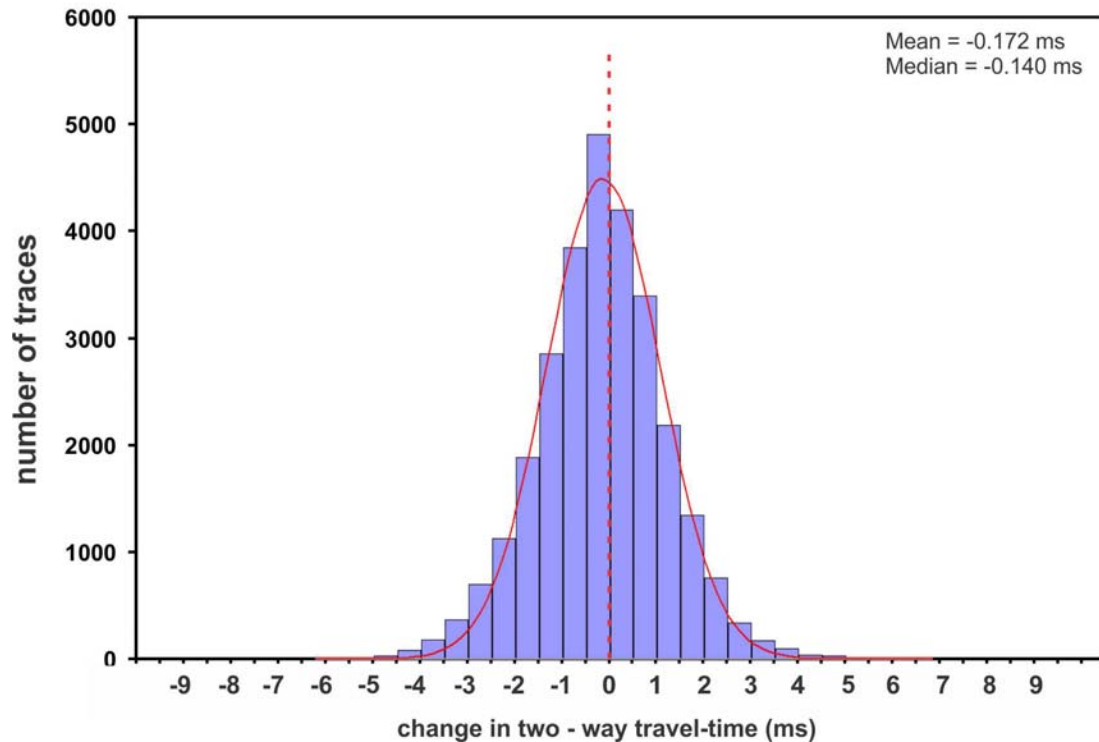


Fig. 17 Observed timeshift distribution and fitted Gaussian curve on a single horizon showing repeatability noise on the Top Utsira Sand reflector from 1994 (baseline) to 2006. Dotted line denotes zero change.

The mean and median values of this distribution are slightly negative reflecting slight ‘static’ time-shifts between the 1994 and 2006 surveys (it is notable that this negative timeshift is the opposite of what would be observed if CO₂ or a pressure anomaly had migrated into the overburden). Because the Utsira time-shift analysis described above looks at changes over a travel-time interval, any ‘static’ timeshifts will show equally at the top and base of the interval and so will be cancelled to zero. The Gaussian curve in Fig. 17, adjusted to a mean of zero, can therefore be reasonably taken as a realistic measure of travel-time noise distribution for the reservoir.

Convolving the noise-free reservoir responses (Fig. 16) with the noise distribution (Fig. 17) gives the calculated real reservoir response for ΔP values of 0.1, 1 and 5 MPa (Fig. 18).

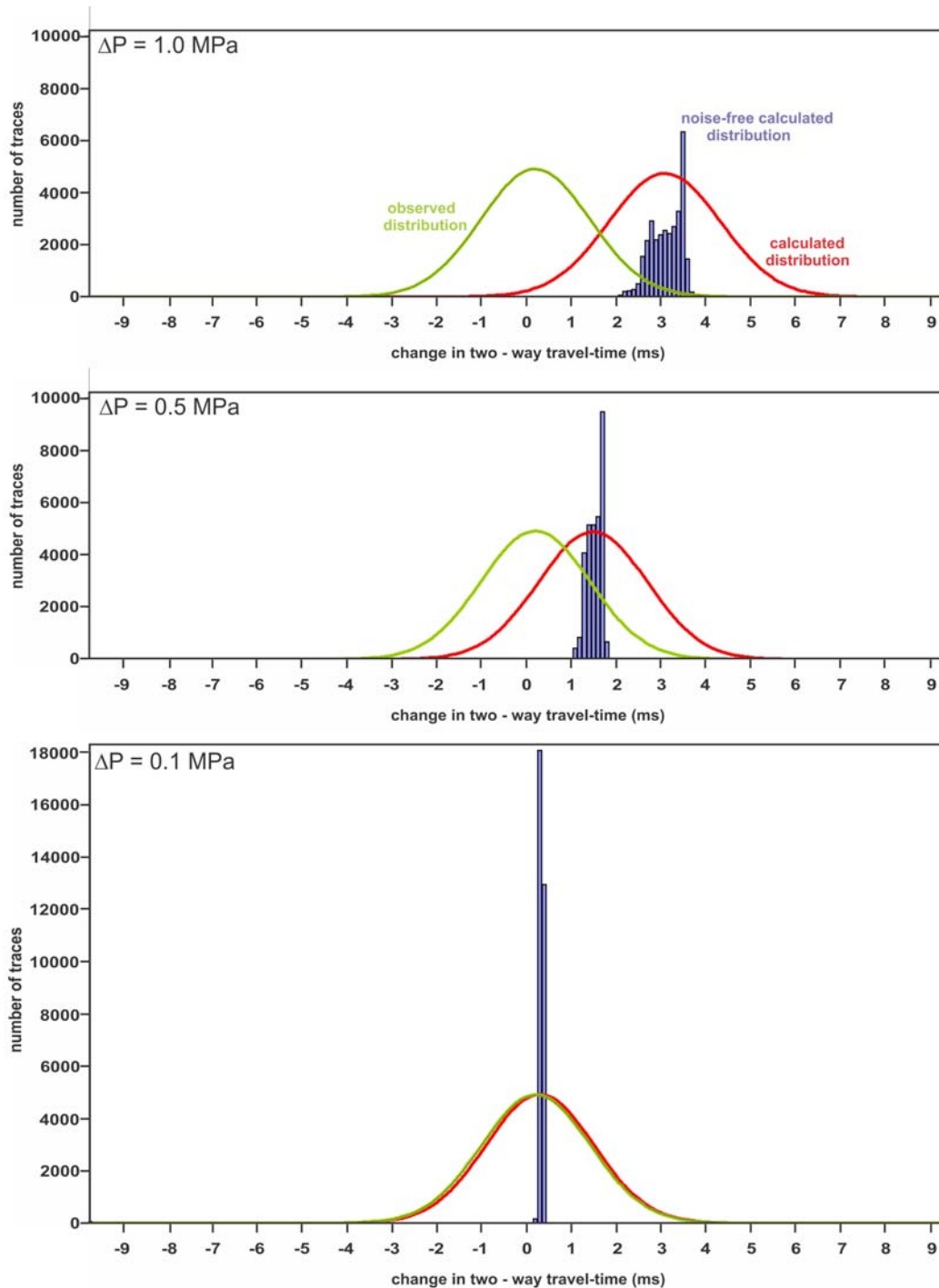


Fig. 18 Reservoir timeshift responses for a range of pressure increase: calculated noise-free reservoir response (blue bars); calculated reservoir response by convolving noise-free response with repeatability noise in Fig. 17 (purple); observed time-shift response (green). a) $\Delta P = 0.1$ MPa b) $\Delta P = 0.5$ MPa c) $\Delta P = 1.0$ MPa.

Comparison of the calculated reservoir responses with the observed time-shifts show a good match of the observed symmetrical spread. In terms of the mean and median values the distributions show a clear mismatch for the 1MPa and 0.5 MPa cases. Even the 0.1MPa case shows a higher mean time-shift than actually observed, which is consistent with true pressure increase less than 0.1 MPa (1 bar).

5.4 Uncertainty

The forgoing analysis depends critically on the sensitivity of the reservoir seismic velocity to changes in formation pressure. Previous work (e.g. Arts et al. 2004) has shown that, in terms of its seismic properties, the virtually unconsolidated Utsira Sand is extremely sensitive to replacing pore-water by CO₂, with a V_p reduction of > 30%. It is reasonable to assume that this high sensitivity will also be evident in its response to changes in pressure. Combining this with the considerable reservoir thickness (up to ~300 m) gives the potential for significant and measurable time-lapse travel-time changes. The presence of noise paradoxically provides a useful statistical tool in providing a readily measurable distribution about the true time-shift mean.

There is some field experience however (e.g. Eiken and Tøndel 2005; White et al. 2011) that the pressure sensitivity of real-world reservoirs is less than indicated by laboratory measurements. Eiken and Tøndel present convincing evidence that velocity decrease in the Troll Ost reservoir is up to 2 – 3 times lower than predicted by laboratory measurements. The reasons for this are unclear, but it might be that microfracturing or other disaggregation processes within the de-stressed cores decrease the strength of rock frame compared to the *in situ* reservoir. An uncemented sand such as the Utsira, might be less affected in this way. Its elastic properties depend almost entirely on grain-to-grain frictional forces which relate directly to the effective stress and it would likely have properties closer to the (weakened) core samples than would a more lithified *in situ* reservoir. Notwithstanding this, we can apply the Eiken and Tøndel reduced sensitivity factor of 2-3 to our data. Taking an average reservoir thickness of 235 m, and an average time-shift to 2006 of 0.175 ms (Fig. 14), the reduced pressure sensitivity assumption would give a pressure increase of between 0.12 and 0.17 MPa. This is still very low, and consistent with little or no flow compartmentalisation within the reservoir (Fig. 5).

Mechanical ‘inflation’ of the reservoir due to increased pore-pressure has been observed directly at In Salah, via measured ground displacement, albeit with much a higher pore pressure rise (Mathieson et al. 2011). As outlined above, increase in actual reservoir thickness depends on the rather poorly-constrained pore compressibility. For typical pore compressibilities the inflation effect is very small, but in an unconsolidated sand such as the Utsira it might be significantly larger (Erik Lindeberg pers. comm.). This effect operates in the opposite sense to the reduced pressure sensitivity and, if significant, would tend to increase time-shifts for a given pressure change. Inferred pressure increases would therefore be rather smaller than reported above.

6. Flow barriers

The very small time-shifts observed on the seismic data provide compelling evidence that only a very small pressure increase has occurred in the Utsira reservoir up to 2006. At distances greater than about 1 km from the injection point ΔP is significantly less than 0.1 MPa (1 bar). Comparing this with the calculated pressures from the flow model (Fig. 5) indicates that strong flow compartmentalisation in the reservoir is unlikely. This pressure behaviour is consistent with the models which have a flow boundary either at the reservoir limit (40 km) or even beyond. In other words, based

on the current data, the Utsira reservoir may either be closed or open but shows no evidence of internal flow compartmentalisation. The current dataset cannot discriminate between these two cases: the pressure field is not yet ‘seeing’ as far as the reservoir edge. Continued injection and progressive pressure buildup might eventually allow the nature of the reservoir boundaries to be discerned i.e. the degree to which fluid flow can take place out of the reservoir itself.

The lack of internal flow compartmentalisation is consistent with the fact that the Utsira Sand shows no evidence of significant faulting (Fig. 2). Identifiable faults or fractures are thought to have throws of less than about a metre and so would not have any sealing capacity due to shale smearing. The reservoir is also dominantly sandy on a regional scale. Thin mudstone barriers within the sand are notably laterally impersistent and allow regional hydraulic connectivity.

7. Conclusions

4D seismic datasets are used to measure pressure changes in the Utsira Sand at Sleipner. Outside of the CO₂ injection plume footprint the data provide strong evidence for only very small time-lapse travel-time changes. These are consistent with pressure increases up to 2006 of less than 0.1 MPa (1 bar) at distances between 500 and 4000 m from the injection point.

From comparison with numerical flow models it is clear that this very low average pressure increase indicates an absence of significant internal flow compartmentalisation within the currently exploited storage reservoir. This is also consistent with the lack of significant faulting observed in the reservoir. It is not possible at the current time however to determine whether the stratigraphical boundary at the depositional limit of the Utsira Sand is acting as a flow barrier or not.

The current study suggests that time-shift mapping using 4D seismic is potentially a useful indicator of reservoir pressure change. This is strongly assisted by the statistical properties of the 3D datasets where many thousands of traces containing repeatability noise create systematic scatter about the true mean. The method will be most effective with thick, poorly-consolidated reservoirs whose mechanical properties are particularly sensitive to changes in effective stress. At Sleipner, injecting rather less than 1 Mt/year, the methodology is close to its sensitivity limits. However large-scale future injection projects, injecting many tens of millions of tonnes of CO₂ at rates of several Mt/year will induce larger and more extensive pressure perturbations. In these circumstances the methodology should prove to be a robust and effective way of mapping reservoir pressure increase.

ACKNOWLEDGEMENTS

This publication has been produced with support from the CO2ReMoVe Project and the BIGCCS Centre, whom we thank for permission to publish. CO2ReMoVe is funded by the EU 6th Framework Programme and by industry partners BP, ConocoPhillips, ExxonMobil, Statoil, Schlumberger, Total, Vattenfall and Wintershall. BIGCCS is part of the Norwegian research program *Centres for*

Environment-friendly Energy Research (FME) and is funded by the Research Council of Norway and an industrial consortium: Aker Solutions AS, ConocoPhillips Skanadinavia AS, Det Norske Veritas AS, Gassco AS, GdF Suez, Hydro Aluminium AS, Shell Technology Norway AS, Statkraft Development AS, Statoil Petroleum AS and TOTAL E&P Norge AS. The authors publish with the permission of the Executive Director, British Geological Survey (NERC).

REFERENCES

- Alnes, H., Eiken, O., Nooner, S., Sasagawa, G., Stenvold, T., Zumberge, M. 2011. Results from Sleipner gravity monitoring: updated density and temperature distribution of the CO₂ plume. Proceedings of the GHGT-10 Conference. Energy Procedia 4, 5504 - 5511.
- Arts, R., Eiken, O., Chadwick, R.A., Zweigel, P., Van Der Meer, L., Kirby, G.A. 2004. Seismic Monitoring at the Sleipner underground CO₂ storage site (North Sea). In: Baines, S., Gale, J., Worden, R.J. (Eds) Geological storage for CO₂ emissions reduction. Spec. Pub. Geol. Soc. Lond. 233, 181 - 191.
- Arts, R.J., Chadwick, R.A., Eiken, O., Thibeau, S., Nooner, S. 2008. Ten years' experience of monitoring CO₂ injection in the Utsira Sand at Sleipner, offshore Norway. First Break 26, 65 – 72.
- Baklid, A., Korbøl, R., Owren, G. 1996. Sleipner Vest CO₂ disposal, CO₂ injection into a shallow underground aquifer. SPE paper 36600, presented at 1996 SPE Annual Technical Conference and Exhibition, Denver Colorado, USA, 6-9 October 1996.
- Benson, S.L., Cook, P. J., Anderson, J., Bachu, S., Nimir, H. B., Basu, B., Bradshaw, J., Deguchi, G., Gale, J., von Goerne, G., Heidug, W., Holloway, S., Kamal, R., Keith, D., Lloyd, P., Rocha, P., Senior, W., Thomson, J., Torp, T., Wildenborg, A., Wilson, M., Zarlenga, F., Zhou, D. 2005. Chapter 5: Underground Geological Storage. In: Metz, B., Davidson, O. Meyer L., de Coninck H.C. (Eds) IPCC (Intergovernmental Panel on Climate Change): Special Report on Carbon Dioxide Capture and Storage. Cambridge University Press, Cambridge, United Kingdom, 440 pp.
- Chadwick, R.A., Arts, R., Eiken, O., Kirby, G.A., Lindeberg, E., Zweigel, P. 2004a. 4D seismic imaging of an injected CO₂ bubble at the Sleipner Field, Central North Sea. In: Davies, R.J, Cartwright, J.A, Stewart, S.A., Lappin, M., Underhill, J.R. (Eds) 3-D Seismic Technology: Application to the Exploration of Sedimentary Basins. Mem. Geol. Soc. Lond. 29, 305-314.
- Chadwick, R.A., Holloway, S., Brook, M., Kirby, G.A. 2004b. The case for underground CO₂ sequestration in northern Europe. In: Baines, S., Gale, J., Worden, R.J. (Eds) Geological Storage for CO₂ emissions reduction. Spec. Pub. Geol. Soc. Lond. 233, 17 - 28.

- Chadwick, R.A., Arts, R., Eiken, O. 2005. 4D seismic quantification of a growing CO₂ plume at Sleipner, North Sea. In: Dore, A.G. & Vining, B. (Eds) Petroleum Geology: North West Europe and Global Perspectives - Proceedings of the 6th Petroleum Geology Conference. Petroleum Geology Conferences Ltd. Published by the Geological Society, London, 1385 – 1399.
- Chadwick, R.A., Arts, R., Bernstone, C., May, F., Thibeau, S., Zweigel, P. 2008. Best Practice for the Storage of CO₂ in Saline Aquifers. (Keyworth, Nottingham: British Geological Survey Occasional Publication No. 14.) ISBN: 978-0-85272-610-5, 277 pp.
- Corey, A.T. 1954. The interrelation between Gas and Oil Relative Permeabilities. Producers Monthly, November 1954, 38-41.
- Eberhart-Phillips, D., Han, D-H., Zoback, M.D. 1989. Empirical relationships among seismic velocity, effective pressure, porosity and clay content in sandstone. Geophysics 54, 82-89.
- Ehlig-Economides, C.A., Economides, M.J. 2010. Sequestering carbon dioxide in a closed underground volume, Journ. Pet. Sci. Eng. 70, 123-130.
- Eiken, O., Tondel, R. 2005. Sensitivity of time-lapse seismic data to pore pressure changes: is quantification possible? The Leading Edge, December 2005, 1250 – 1254.
- Freeze, R. A., Cherry, J. A. 1979. Groundwater. London: Prentice-Hall.
- Han, De-h., Nur, A., Morgan, D. 1986. Effects of porosity and clay content on wave velocities in sandstones: Geophysics 51, 2093-2107.
- Harrington, J.F., Noy, D.J., Horseman, S.T., Birchall, D.J., Chadwick, R.A. 2010. Laboratory study of gas and water flow in the Nordland Shale, Sleipner, North Sea. In: Grobe, M., Pashin, J., Dodge, R. (Eds) Carbon Dioxide Sequestration in Geological Media. Spec. Pub. Am. Assoc. Pet. Geol. 59, 521 – 543.
- Holloway, S. 2001. Storage of Fossil Fuel-Derived Carbon Dioxide Beneath the Surface of the Earth. Ann. Rev. En. and Env. 26,145-166.
- Hovorka, S. 2005. Testing efficiency of CO₂ storage in the subsurface: Frio Brine pilot project. In: Rubin, E. S., Keith, D. W., Gilboy, C. F. (Eds) Proceedings of the 7th International Conference on Greenhouse Gas Control Technologies, Volume 2. Contributed papers and panel discussion, Elsevier, Oxford, 1361–1366.
- IPCC 2007. Climate Change 2007: The Physical Science Basis, Summary for Policymakers. <http://www.ipcc.ch/SPM2feb07.pdf>
- Kikuta, K., Hongo, S., Tanase, D., Ohsumi, T. 2005. Field test of CO₂ injection in Nagaoka, Japan. In: Rubin, E. S., Keith, D. W., Gilboy, C. F. (Eds) Proceedings of the 7th International Conference on Greenhouse Gas Control Technologies, Volume 2. Contributed papers and panel discussion, Elsevier, Oxford, 1367–1372.

- Korbøl, R., Kaddour, A. 1995. Sleipner Vest CO₂ disposal – injection of removed CO₂ into the Utsira Formation. In: Kondo, J., Inui, T., Wasa, K. (Eds). Proceedings of the second International Conference on Carbon Dioxide Removal, Kyoto 24-27 October 1994. Pergamon, 519-512.
- Mathieson, A., Midgley, J., Wright, I., Saoula, N., Ringrose, P. 2011. In Salah CO₂ storage JIP: CO₂ sequestration monitoring and verification technologies applied at Krechba, Algeria. *Energy Procedia* 4, 3596 – 3603.
- Onuma, T., Ohkawa, S. 2008. Detection of surface deformation related with CO₂ Injection by DInSAR at In Salah, Algeria, Proceedings of the 9th International Conference on Greenhouse Gas Control Technologies, 2177–2184.
- Pruess, K. 2005. ECO2N: A TOUGH2 Fluid Property Module for Mixtures of Water, NaCl, and CO₂. Lawrence Berkeley National Laboratory Report LBNL-57952.
- Riddiford, F.A., Tourqui, A., Bishop, C.D., Taylor, B., Smith, M. 2003. A cleaner development: the In Salah Gas project, Algeria. In: Gale, J., Kaya, Y. (Eds) *Greenhouse Gas Control Technologies*, Volume 1, 595-600, Pergamon, Amsterdam.
- White, D.J. for the Weyburn Geophysical Monitoring Team. 2011. Geophysical monitoring of the Weyburn CO₂ flood: Results during 10 years of injection. *Energy Procedia* 4 (2011), 3628 – 3635.
- Wilson, M., Monea, M. 2004. IEA GHG Weyburn CO₂ Monitoring & Storage Operation Summary Report 2000 - 2004. Petroleum Technology Research Centre, Regina, SK, Canada, 273 pp.
- Wiprut, D. & Zoback, M.D. 2002. Fault reactivation, leakage potential and hydrocarbon column heights in the northern North Sea. In: Koestler, A.G. & Hunsdale, R. (eds) *Hydrocarbon Seal Quantification*. Norwegian Petroleum Society (NPF) Special Publication, Elsevier, Amsterdam, 11, 203–219.
- Wyllie, M.R.J., Gregory, A.R., Gardner, G.H.F. 1958. An experimental investigation of factors affecting elastic wave velocities in porous media. *Geophysics* 23, 459-493.
- Xue, Z., Ohsumi, T. 2004. Seismic wave monitoring of CO₂ migration in water-saturated porous sandstone. *Exploration Geophysics* 35, 25-32.
- Zhang, J.J., Bentley, R. 1999. Change of bulk and shear moduli of dry sandstone with effective pressure and temperature. CREWES Research Report, Volume 11. Consortium for Research in Elastic Wave Exploration Seismology, University of Calgary. [<http://www.crewes.org>]
- Zimmer, M., Prasad, M., Mavko, G. 2002. Pressure and porosity influences on V_p-V_s ratio in unconsolidated sands. *The Leading Edge*, February 2002, 178-183.
- Zweigel, P., Arts, R., Lothe, A.E., Lindeberg, E.R.G. 2004. Reservoir geology of the Utsira Formation at the first industrial-scale underground CO₂ storage site (Sleipner

area, North Sea). In: Baines, S., Gale, J., Worden, R.J. (Eds) Geological Storage for CO₂ emissions reduction. Special Publication of the Geological Society, London, 233, 165 - 180.